Thermal activation of crack-tip plasticity: The brittle or ductile response of a stationary crack loaded to failure

Alexander Hartmaier*
Max Planck Institute for Metals Research, Heisenbergstr. 3, 70569 Stuttgart, Germany

Peter Gumbsch
Fraunhofer-Institut für Werkstoffmechanik, Wöhlerstrasse 11, 79108 Freiburg, Germany
and Universität Karlsruhe, Institut für Zuverlässigkeit von Bauteilen und Systemen, Kaiserstrasse 12, 76131 Karlsruhe, Germany
(Received 4 June 2004; revised manuscript received 6 August 2004; published 20 January 2005)

Metals with a body centered cubic crystal structure, like tungsten, exhibit a pronounced semibrittle regime at intermediate temperatures. In this regime their fracture toughness strongly depends on loading rate and temperature. Crack-tip plasticity has been studied with two-dimensional numerical simulations on different length scales. The method of discrete dislocation dynamics has been employed to test various assumptions made on the deformation mechanisms and the origin of the strong loading rate and temperature dependence of fracture toughness in this regime. A continuum elasticity-viscoplasticity model capable of describing larger plastic deformations yields complementary information with respect to the discrete dislocation method. Despite of their fundamental differences, both simulations consistently show that crack-tip plasticity can be described as a time-dependent microplastic deformation with well-defined activation energy and that the blunting of the crack tip plays an important role for the transition from semibrittle to ductile behavior. Based on general findings of the numerical simulations an Arrheniuslike relation between loading rate and temperature at points of constant fracture toughness is derived. This scaling relation shows the dominance of dislocation mobility as the rate limiting factor for fracture toughness and for the brittle-to-ductile transition itself. The results of our simulations are also consistent with experimental data gathered on tungsten single crystals. Thus, the proposed scaling relation can be used to predict fracture toughnesses in a wide range of temperatures and loading rates, based on only a small number of experiments.

DOI: 10.1103/PhysRevB.71.024108 PACS number(s): 62.20.Mk, 46.50.+a, 62.20.Fe, 46.15.−x

I. INTRODUCTION

The investigation of the failure of materials is one of the main tasks of materials science, because the failure properties of a material determine the limits of its technological applicability. General failure properties of a material, classified into brittle and ductile failure, as well as the material's reaction to pre-existing flaws are important engineering parameters. Materials with a face centered cubic structure usually show ductile behavior at all temperatures and deformation rates. Materials with stronger interatomic forces like body centered cubic metals, intermetallic phases, semiconductors, and also ionic crystals often show a transition between brittleness at low temperatures or high deformation rates and ductility at high temperatures or low deformation rates.[1] Materials with a non-negligible dislocation density before testing usually exhibit a more or less pronounced semibrittle regime, where the fracture toughness rises steadily with the temperature. The testing of virtually defect-free specimens like silicon or alumina single crystals reveals an exceptionally sharp brittle-to-ductile transition (BDT).[1] Despite these peculiarities, especially silicon has often been chosen as model material for studies of fracture and the BDT, because large, defect-free single crystals are easily available. While the main part of the work on the BDT has been conducted by loading a stationary crack until crack advance occurs, Gally and Argon[2] have performed complementary experiments by running a crack against a temperature gradient until the BDT occurs and the crack stops. Both methods are used to reveal material properties like BDT temperature, activated slip systems, etc., and both methods allow the activation energy of the BDT to be assessed. The stationary method, however, seems to be restricted to lower loading rates, while the dynamic crack arrest method yields values for higher loading rates.

Classical discrete-dislocation-based treatments of crack-tip plasticity[3–5] have been restricted to the case where the dislocation population is always in equilibrium, which inherently assumes static or quasistatic loading conditions or very large lattice friction stresses. In this case, closed form solutions of the force balancing equations can be derived.[4,6] However, under such equilibrium conditions the ductility or brittleness of a material is completely determined by its ability or inability to generate dislocations below the failure stress.[3] The importance of dislocation mobility for fracture behavior under nonstatic loading conditions has been pointed out by Hirsch *et al.*[7]

Quasistatic loading conditions or equilibrium of the dislocations is also implicitly assumed in continuum plasticity or continuum crystal-plasticity models of crack-tip plasticity.[8–10] In a recent study, dimensional analysis of energy dissipating processes at crack tips is used to describe such processes and their influence on fracture toughness in a general framework.[11] The influence of time-dependent loading conditions on the evolution of a crack-tip plastic zone has been investigated by Nitzsche and Hsia.[12] In this work,

the material close to the crack tip has been described as purely elastic. Around this elastic zone an elastic-viscoplastic material was allowed to relax the elastic strains in a time-dependent manner. This model of crack-tip plasticity exhibits an extremely sharp transition between brittle and ductile behavior. The time-dependent plastic behavior at crack tips has also been modeled analytically,[13,14] which led to expressions for the influence of pre-existing dislocations on the fracture toughness and for the thermal activation of the BDT in silicon.

In the following sections of the present work, a discrete dislocation dynamics model of crack-tip plasticity in engineering materials is developed that assumes a high density of dislocation sources close to the crack tip, and thus easy dislocation nucleation. Such a system is expected to show a smooth transition from brittleness to ductility and thereby a pronounced semibrittle regime. The behavior of this model system under constant loading rates is investigated and general findings of the numerical simulations are put in a theoretical framework. Under these nonequilibrium conditions no closed form solutions can be derived, but it will be shown that the results of numerical simulations can be described in a very general form by a scaling relation for the dependence of fracture toughness on temperature and loading rate. The findings of the discrete dislocation dynamics model of crack-tip plasticity are compared with the results obtained from a continuum elastic-viscoplastic model of the crack-tip region. The results of these two complementary methods confirm the model-independent validity of the scaling relation and allow us to draw further conclusions about the nature of the brittle-to-ductile transition.

II. DISCRETE DISLOCATION MODEL

The model of crack-tip plasticity described below is expected to capture the most important features of fracture processes in real materials. Especially the elastic shielding of a crack tip by dislocations nucleated nearby is taken into account. Due to its simplicity this model is very well suited to be transferred into a numerical simulation scheme. Such numerical simulations of crack-tip plasticity based on discrete dislocation dynamics (DDD) in two dimensions have been developed by Lin and Thomson[15] and have been employed thereafter by several groups. A detailed description of the two-dimensional DDD scheme employed here can be found in Refs. 16 and 17.

A. Geometry

In this work an isotropic elastic medium with a semi-infinite crack subject to pure mode I loading with the stress intensity factor K_a is considered. The load is applied with a constant rate $\dot{K}$. The temperature T is assumed to be constant during the loading process. For simplicity a single slip system is taken into account, considering exclusively slip of edge dislocations on the slip plane with the highest resolved shear stress, which is inclined to the crack plane by an angle of $\varphi = 70.5°$. A sketch of the geometry of the system under consideration is provided in Fig. 1.

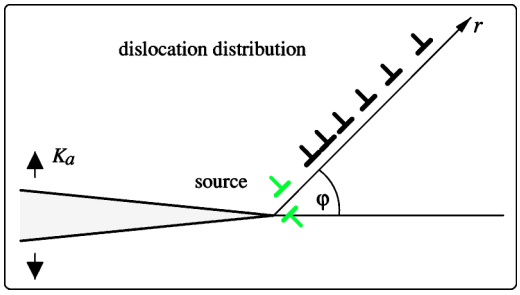

FIG. 1. Sketch of the model system of a crack loaded in mode I with stress intensity factor K_a. Dislocations nucleate at the source position and glide on a single slip plane.

The physical quantities K_a, $\dot{K}$, and T are the external variables determining the state of the model system as well as the state of experimental fracture samples. Together with the material parameters and the sample geometry these external state variables determine fracture toughness.

B. Dislocation activity

The rate of plastic deformation is limited either by the dislocation nucleation rate or by the dislocation velocity v_d. Therefore both phenomena are highlighted in this section.

The criterion for the nucleation of a new dislocation is that the resolved shear stress at the source position (see Fig. 1) must be sufficiently large to repel a dislocation from the crack-tip against the image forces stemming from the free surface. The source position is at a distance of 30 Burgers vectors (or 8.2 nm) from the crack tip. In this work, only the shielding dislocation is nucleated while the blunting (anti-shielding) dislocation that is absorbed by the crack within short characteristic times is neglected. For a larger number of dislocation sources it is useful to take these dislocations into account,[18] however, in this work the blunting of the crack-tip is only considered in the failure criterion, as described in the next section. In this simple model, the distance between crack-tip and dislocation source determines the critical stress intensity factor at which the first dislocation nucleation occurs. Due to elastic shielding, such a dislocation nucleation causes the local stress intensity factor at the crack tip to drop.[15] As the dislocation moves away from the crack tip and the *applied* stress intensity factor is increased, also the *local* stress intensity factor rises again and, finally, assumes a maximum immediately before a new dislocation is nucleated. This local maximum in the stress intensity factor is the critical stress intensity factor for dislocation nucleation, which due to the elastic interaction of incipient and existing dislocations rises in the course of the simulation (cf. Fig. 2). The employed nucleation criterion causes dislocation nucleation to occur easily, i.e., without energy barrier, and homogeneously along the crack front, which refers to the case of a high density of imperfections at the crack front acting as dislocation sources.

Under this condition one finds that the nucleation rate is limited by the speed at which previously nucleated dislocations leave the crack-tip region.[4,5] In body centered cubic materials and also in semiconductors the velocity of both,

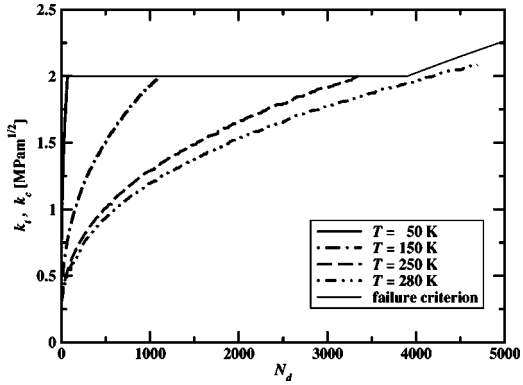

FIG. 2. Local stress intensity factor k_t (thick lines) plotted versus the number of dislocations N_d for material WN in Table I. The loading rate is $\dot{K}=0.1$ MPa$\sqrt{\text{m}}$/s and temperatures are given in the legend. The failure criterion k_c (thin solid line) is plotted for comparison.

screw[19,20] and nonscrew[21] dislocations, must be considered to be thermally activated. In most of this work dislocation velocity v_d is described as function of resolved shear stress τ and temperature T by the empirical formulation

$$v_d(\tau,T) = v_0\left(\frac{\tau}{\tau_0}\right)^m \exp\left(-\frac{Q}{k_B T}\right), \tag{1}$$

with the pre-exponential factor v_0, the normalization stress τ_0, the stress exponent m, and the activation energy Q (k_B is the Boltzmann constant). The mobility of nonscrew dislocations in tungsten is described by Eq. (1) using a temperature dependent stress exponent of the form $m(T)=a/T+b$.[21]

A more rigorous thermodynamical treatment of dislocation mobility yields[22]

$$v_d(\tau,T) = v_0 \exp\left(-\frac{Q[1-(\tau/\tau_0)^m]^n}{k_B T}\right) \tag{2}$$

for the dislocation velocity, where a second stress exponent n is introduced and τ_0 is interpreted as the Peierls stress. This formulation is mainly used to describe screw dislocation mobility in body centered cubic metals. The material parameters employed here are given in Table I. All numerical simulations represented in this work are performed with Young's modulus $E=393.9$ GPa, Poisson ratio $\nu=0.29$, and norm of the Burgers vector $b=0.274$ nm.

C. Failure model

To determine the fracture toughness from the numerical simulations, a failure criterion needs to be introduced. This failure criterion is based on a critical value k_c of the local stress intensity factor. In the case of a sharp crack tip this critical stress intensity factor is expressed in the form k_c = constant, following the Griffith criterion, which only depends on elastic material parameters and the material's surface energy. In this work the critical stress intensity factor for a sharp crack tip is set to $k_{c,s}=2$ MPa$\sqrt{\text{m}}$, corresponding to the low temperature fracture toughness of tungsten single crystals.[25]

The blunting of the crack tip by a number of N_d dislocations yields a notch radius $r_t=b/2N_d \sin\varphi$, where φ is the inclination angle of the slip plane. Failure of a blunt notch is assumed to occur when the tensile stress in front of the crack tip reaches the cohesive strength R_c of the material. At this point a sharp crack will be renucleated that immediately propagates through the material, because $k_{c,s}$ is exceeded. The cohesive strength criterion for the blunted crack can also be formulated in terms of a critical local stress intensity factor, which yields

$$k_{c,b} = \frac{R_c}{2}\sqrt{\pi r_t} = \frac{R_c}{4}\sqrt{2\pi b N_d \sin\varphi}. \tag{3}$$

For crack tips with a small blunting radius, where $k_{c,b}$ is smaller than the critical stress intensity factor for a sharp crack, obviously the larger value must be employed. Therefore the combined failure criterion is written as

$$k_c = \begin{cases} k_{c,s} & \text{if } N_d < N_d^{\text{crit}} \\ k_{c,b} & \text{else} \end{cases}, \tag{4}$$

where $N_d^{\text{crit}}=8k_{c,s}^2/(\pi b R_c^2 \sin\varphi)$ is the critical number of dislocations for the transition between failure of the sharp or blunt cracks, respectively. This failure model is qualitatively consistent with atomistic studies of renucleation of sharp cracks from blunt notches,[26] where it has been found that for small blunting radii the critical stress intensity factor is almost constant. The failure criterion is defined with respect to

TABLE I. Material parameters describing dislocation mobility of nonscrew dislocations [Eq. (1)] and of screw dislocations [Eq. (2)]. The parameters for nonscrew dislocations—marked with WN—are chosen to give a good agreement with the BDT temperatures found in experiment (Ref. 23). The values are based on experimental results from Schadler (Ref. 21) and were changed slightly in comparison to earlier work (Refs. 16, 17, and 24). The parameters for screw dislocations in a $\langle 111\rangle\{110\}$ slip system in tungsten are marked by WS (Ref. 20). The parameters in the last two rows marked with AN (nonscrew) and AS (screw) are employed in a parameter study represented in Fig. 4.

Type	v_0 [m/s]	τ_0 [GPa]	Q [eV]	m	n
WN	$0.32\cdot10^{-8}$	10^{-3}	0.35	450 K/T+3.5	-
WS	3000	1.3	1.8	1	2.8
AN	$0.32\cdot10^{-8}$	10^{-3}	0.3	5, 10	-
AS	3000	0.4, 0.8	0.3	2, 4	1

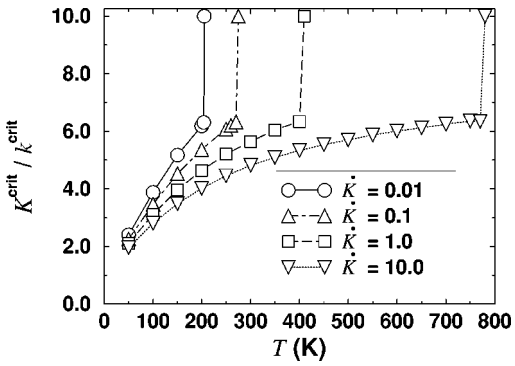

FIG. 3. Relative fracture toughness K_a/k_c as a function of temperature T for different loading rates as given in the legend.

the number of dislocations, because this quantity plays a central role in the following investigations. In this work we define failure of the material as the instance when the failure criterion for the *local* stress intensity factor is met, and refer to the *applied* stress intensity factor at this stage as the fracture toughness K_c.

In Fig. 2 the failure criterion is plotted versus the total number of dislocations together with results from numerical simulations for different temperatures. The numerical results are reproduced by lines connecting the maxima of the local stress intensity factor immediately before a new dislocation is nucleated. It is seen that this critical local stress intensity factor for dislocation nucleation continuously rises during the simulations (as explained above) and finally exceeds the failure criterion k_c. The figure shows further that the failure criterion is only met for the case of a sharp crack tip. If the tip is blunted sufficiently and the failure criterion follows $k_{c,b}$, the local stress intensity factor always stays below the critical value. The temperature at which this occurs defines the BDT temperature. For these simulations a limiting value of $N_d^{\mathrm{crit}}=3900$ has been employed above which crack tip blunting is taken into account. This—rather high—value is chosen because it yields BDT temperatures in good agreement with experimental results on tungsten single crystals.[23] The choice of the limit for the number of dislocations also fixes the rupture strength, which will be discussed in detail in Sec. V. In Fig. 3 the resulting fracture toughnesses are plotted versus the temperature. It is seen that the fracture toughness rises steadily in the semibrittle regime. When the failure criterion changes to the one for a blunted crack tip, the model predicts ductile behavior and the fracture toughness jumps to undefined values. This point marks the BDT, and consequently defines the BDT temperature T_{BDT}, which will be used later to calculate the activation energy for the BDT.

Further details of the dependence of fracture toughness on temperature and loading rate for different dislocation nucleation criteria and different formulations of dislocation velocity are reported elsewhere.[16,17,24] The following chapter is dedicated to the analysis of the force balance of all defects. This force balance is formulated analytically, but depends on results of the DDD simulations, which are needed to evaluate the equations and to derive a scaling relation for loading rate and temperature at points of constant fracture toughness.

III. CRACK-TIP PLASTICITY

The following analysis of crack-tip plasticity is based on the force balance between the different defects in the crack tip region. The mathematical concepts are revisited here for completeness, a more detailed derivation can be found in Ref. 24. Following the treatise of Weertman, Lin, and Thomson,[6] this force balance for an elastic medium containing a crack and a set of dislocations is written as

$$G = g_t + \sum_{j=1}^{N_d} g_d^{(j)}, \tag{5}$$

where g_t is the force on the crack tip, $g_d^{(j)}$ is the force on dislocation j, and G is the total force on all defects. We only consider forces in the direction of crack advance, therefore all quantities here are given as real valued scalars. The total force G is identified with the energy release rate of the crack, which is for pure mode I loading $G=K_a^2(1-\nu^2)/E$. In the same way the force on the crack tip can be written as $g_t = k_t^2(1-\nu^2)/E$, with the local stress intensity factor k_t.

The validity of these equations is strictly proven only for a mode III crack and a population of screw dislocations that is symmetrical with respect to the crack plane.[6] However, numerical simulations show that in the present case, too, this force balance is fulfilled to a very good approximation.[24]

The sum over all dislocations in Eq. (5) cannot be simplified without further restricting assumptions, but the analysis of the results of DDD simulations with a variety of parameters shows that this term can be expressed as a product of powers of the local stress intensity factor and the number of dislocations in the form

$$\frac{E}{1-\nu^2}\sum_{j=1}^{N_d} g_d^{(j)} = K_a^2 - k_t^2 = C\left(\frac{k_t}{k_c}\right)^s N_d^q, \tag{6}$$

with three constants C, s, q.

An unexpected and very general result is that these constants are only functions of the material parameters E, ν, and b, but neither of the external state variables, like loading rate or temperature, nor of the parameters or the formulation of the dislocation velocity law. The interpretation of this finding is that the force balance of the crack-tip region is only a function of the number of dislocations that itself, of course, depends on the state variables and the dislocation velocity law. On the microstructural level, the shielding of the crack tip depends only on the dislocation distribution, given by the number and distances of the dislocations to the crack tip. Therefore, a physical motivation of the finding that the dislocation microstructure—in our confined system—depends only on the number of dislocations, but not independently on state variables or parameters of the dislocation velocity, is that the collective dynamics of the dislocation population depends only on the mutual elastic interaction of the defects, which is completely described by E, ν, and b.[15] Therefore, the dislocation population may reach the same total number of dislocations at different applied loads, but size and structure of the dislocation distribution will nonetheless be similar.

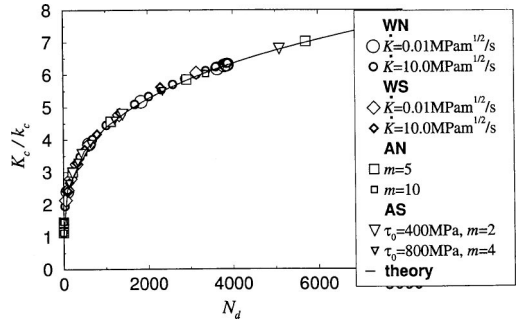

FIG. 4. Fracture toughness as a function of the number of dislocations. The parameters for dislocation mobility refer to Table I. Parameters that are varied are given in the legend. If not stated otherwise, the loading rate is $\dot{K}=1$ MPa$\sqrt{\text{m}}$/s. The theoretical curve according to Eq. (7) is also plotted.

In the formalism used here, the fracture toughness is derived from the right-hand side of Eq. (6) by inserting $k_t=k_c$. This yields

$$K_c = \sqrt{k_c^2 + CN_d^q}, \tag{7}$$

which is only a function of the number of dislocations and the failure criterion. In Fig. 4, where K_c is plotted as a function of N_d for a number of loading rates, temperatures, activation energies, and stress exponents, it is verified that the fracture toughness does not depend on these quantities independently, but only through the number of dislocations. For this parameter study, the failure criterion has been restricted to the case of a sharp crack tip, i.e., $k_c=k_{c,s}$.

A. Scaling relations for crack-tip plasticity

A further general result of the DDD simulations is that the dislocation nucleation rate $\dot{N}_d$ is directly proportional to the velocity of the leading dislocation in the inverse-pileup ahead of the crack tip. The number of dislocations can thus be expressed as a time integral over the velocity of this dislocation. Together with Eq. (1), and by making use of the constant loading rate $\dot{K}=dK_a/dt$ in rewriting the time integral into an integral over the applied stress intensity factor, this gives

$$N_d = \frac{A}{\dot{K}} \exp\left(-\frac{Q}{k_B T}\right) \int_{K_a'=0}^{K_a} \left(\frac{\tau^{(1)}}{\tau_0}\right)^m dK_a', \tag{8}$$

with the proportionality constant A. The separability of the functions containing stress and temperature in the velocity law has been used for the derivation of Eq. (8). For the velocity law in Eq. (2) or a temperature dependent stress exponent, stress and temperature are not separable functions. However, the exponential term can always be extracted, but a temperature dependent term under the integral remains. In any case, the integral cannot be evaluated further at this stage, because the dependence of $\tau^{(1)}$ on K_a is unknown. In the further, the integral is written as an unknown function $F(K_a)$. Inserting Eq. (8) at $K_a=K_c$ into Eq. (7) and separating all terms containing K_c yields

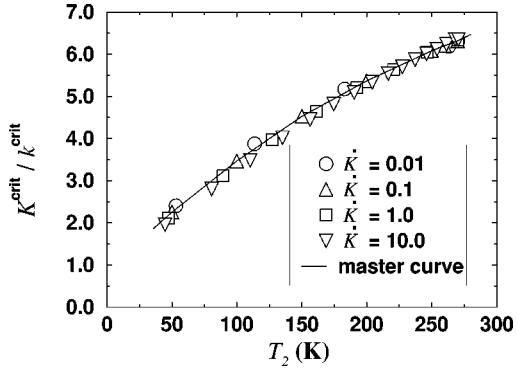

FIG. 5. Fracture toughness-temperature plot with rescaled temperature axis [Eq. (10)] for material WN (Table (1)). The basis loading rate is $\dot{K}_2=0.1$ MPa$\sqrt{\text{m}}$/s, all loading rates are given in units of MPa$\sqrt{\text{m}}$/s. The master curve is given as a mere visual guide.

$$\frac{(K_c^2 - k_c^2)^{1/q}}{C^{1/q} F(K_c)} = \frac{A}{\dot{K}} \exp\left(-\frac{Q}{k_B T}\right). \tag{9}$$

This implicit expression of the fracture toughness K_c as a function of the state variables $\dot{K}$ and T is at the same time an Arrheniuslike relation for points of constant fracture toughness, where the left-hand side of the equation is constant. Such an Arrheniuslike relation has been postulated already in earlier work[17] as a hypothesis to explain the observed scaling behavior of experimental and numerical results. All combinations (K_i, T_i), $i \in \{1,2,3,\ldots,\}$, of loading rates and temperatures that lead to the same fracture toughness—and consequently to the same total number of dislocations—must fulfill the relation

$$T_2 = \left(\frac{k_B}{Q} \ln \frac{\dot{K}_1}{\dot{K}_2} + \frac{1}{T_1}\right)^{-1}. \tag{10}$$

This relation can be used to rescale the temperature axis of results obtained for different loading rates and activation energies, thus projecting these results on a single master curve. The scaling is demonstrated here in Fig. 5 for material WN (Table I), which shows that results obtained for different parameters re-scale on a single master curve. Further examples for different velocity laws can be found in Refs. 17 and 24, where also the validity of this scaling relation for experimental data of three-point bending tests on tungsten single crystals has been reported.

The scaling procedure defines the apparent activation energy for crack-tip plasticity Q_{scal}. The derivation above has shown that this apparent activation energy for crack-tip plasticity is identical to the activation energy for dislocation motion if stress and temperature contribute to the dislocation velocity as separable functions. If this condition is not met, however, the slight temperature dependence of the function $F(K_c)$ in Eq. (9) causes the apparent activation energy for crack-tip plasticity Q_{scal} used in the scaling relation to be somewhat smaller than the activation energy for dislocation motion. Furthermore, the quality of the scaling onto a single

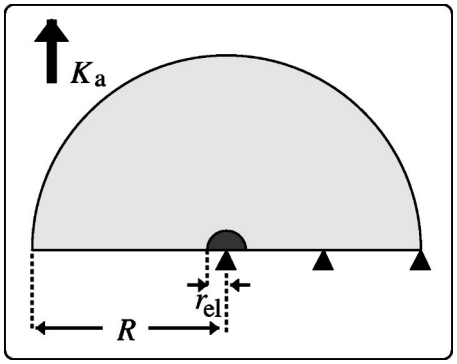

FIG. 6. 2D finite element model to describe crack-tip plasticity and the BDT. The viscoplastic zone is shaded light gray, the elastic zone dark gray. Plane strain is assumed for all elements. Details of the model are given in the text.

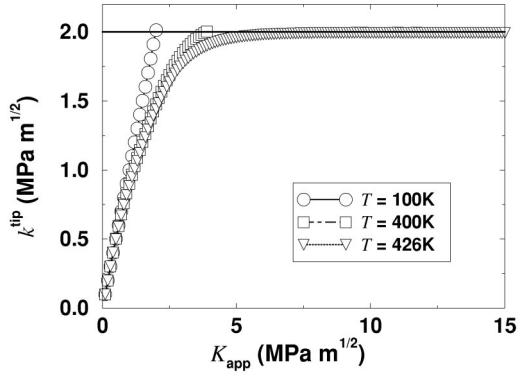

FIG. 7. Local stress intensity k_t versus applied stress intensity K_a for different temperatures T. The loading rate is $\dot{K}$ = 1.0 MPa m$^{1/2}$/s. The critical local stress intensity is k_c = 2.0 MPa m$^{1/2}$ (thick lines).

master curve is inferior to the case of a constant stress exponent.[17] The reduction amounts to $Q_{scal}=0.17$ eV for tungsten nonscrew dislocations (WN with $Q=0.35$ eV) and to $Q_{scal}=1.4$ eV for screw dislocations (WS with $Q=1.8$ eV).

The scaling relation has been derived here based on the force balance of discrete defects in the crack-tip region. In the following section its validity is demonstrated on a continuum model that is based on different assumptions and simplifications.

IV. CONTINUUM PLASTICITY MODEL

A two-dimensional (2D) finite element model of the crack-tip region is set up, with a purely elastic zone around the crack tip and an elastic-viscoplastic material elsewhere. Compared with the 2D-DDD method the viscoplasticity description is not limited to single slip planes and small plastic strains. In this sense the DDD model and the continuum model represent two extreme cases of descriptions of crack-tip plasticity. The constitutive law of the continuum plasticity description captures activity on multiple slip planes and cross slip as well as dislocation multiplication in an average sense. The model employed here has been developed by Nitzsche and Hsia[12] to describe the sharp BDT of silicon single crystals.

The geometry of the finite element model employed here is a half-circle of radius R (see Fig. 6). Following Ref. 12, the linear elastic displacements of a pure K_I field are applied as nodal displacements at the outer boundary of the model. Free boundary conditions are active on the left-hand side of the symmetry axis, thus being the free crack plane. Perpendicular nodal displacements are blocked along the right-hand side of the symmetry axis, which yields a mirror symmetry in this part. Plane strain conditions are assumed for all elements. The size r_{el} of the elastic zone surrounding the crack tip amounts to 1 μm and is smaller than the crack length R by a factor of 20.

The material behavior outside the elastic zone is rate-dependent viscoplastic. The strain rate $\dot{\varepsilon}$ follows the Orowan law

$$\dot{\varepsilon} = b\rho_m v_d(\tau, T), \tag{11}$$

in which the dislocation velocity according to Eq. (1) is inserted. This yields the power law

$$\dot{\varepsilon} = b\rho_m v_0 \exp\left(-\frac{Q}{k_B T}\right)\left(\frac{\tau}{\tau_0}\right)^{m(T)} = \dot{\varepsilon}_0(T)\left(\frac{\tau}{\tau_0}\right)^{m(T)}, \tag{12}$$

for the the strain rate, where the temperature dependent stress exponent m is defined as $m(T)=\alpha/T+\beta$. The form of this viscoplastic law resembles the common formulations of power law creep. The material parameters are the same as those for the DDD simulations (see Table I) to ensure the comparability of both methods. The density ρ_m of mobile dislocations $\rho_m=3.5\times10^{10}$ m/m^3 is assumed, because this value gives good agreement of the numerical results for the BDT temperatures with experimental data.[23] If the dislocation density is higher, the BDT occurs at lower temperatures and *vice versa*. The value of ρ_m employed here is somewhat higher than that determined by x-ray topography of specimen material of the cited work ($\rho_{exp}=5.0\times10^9$ m/m^3).[27,28]

Similar to the 2D-DDD model, the numerical simulations start with a zero applied stress intensity K_I, which is raised with a constant rate $\dot{K}$. The temperature is assumed to be constant during each simulation. The applied load is increased in equidistant steps ΔK_a. The system is allowed to relax for the time $\Delta t=\Delta K_a/\dot{K}$ after each step. The convergence of the finite element calculation is verified by controlling the relaxation of the nodal forces.

The simulation is stopped either when the failure criterion for a sharp crack is met or when the applied load of K_a = 40 MPa m$^{1/2}$ is reached. In the latter case, the local stress intensity factor stays constant below the critical value although the applied load is rising, as seen in Fig. 7. The first occurrence of such a flat K_a-k_t-curve defines the BDT.

Fracture toughness versus temperature is plotted for several loading rates in Fig. 8. The fracture toughness remains almost constant up to the BDT temperature, where it rises sharply. These results are consistent with the observations of Nitzsche and Hisa.[12] The apparent activation energy of the BDT of $U_{bdt}=0.17$ eV, derived from an Arrhenius analysis of the BDT temperature, is significantly lower than the activation energy of the underlying viscoplastic deformation law ($Q=0.35$ eV), but on the same order as the apparent activa-

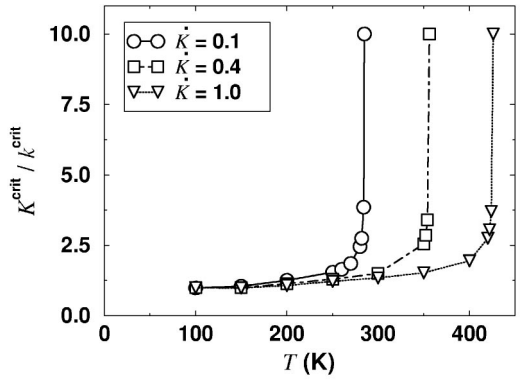

FIG. 8. Fracture toughness K_c versus temperature T as calculated with the 2D finite element model. The density of mobile dislocations is $\rho_m = 3.5 \times 10^{10}$ m/m^3, the loading rate $\dot{K}$ is given in MPa m$^{1/2}$/s.

tion energy for crack-tip plasticity obtained from the scaling of the DDD results (cf. Fig. 10).

The plastic strain at the boundary at radius R remains below 5% up to applied loads of $K_a = 20$ MPa m$^{1/2}$, which provides a justification for applying the elastic K-field solution as boundary condition.

A detailed analysis of the spatial distribution of the plastic strain at different stages of the loading reveals that the plastic zone starts to develop close to the elastic zone around the crack tip in the region between 45° to 135°, where the highest stresses are found [Fig. 9(a)]. During plastic relaxation these high stress levels are diminished and the plastic zone expands continuously around the elastic zone [Fig. 9(b)]. Finally, the location of the highest plastic strain moves towards the intersection of the elastic zone with the crack plane [Figs. 9(c) and 9(d)].

During the simulations where the critical stress intensity at the crack tip is exceeded, the expansion of the plastic zone

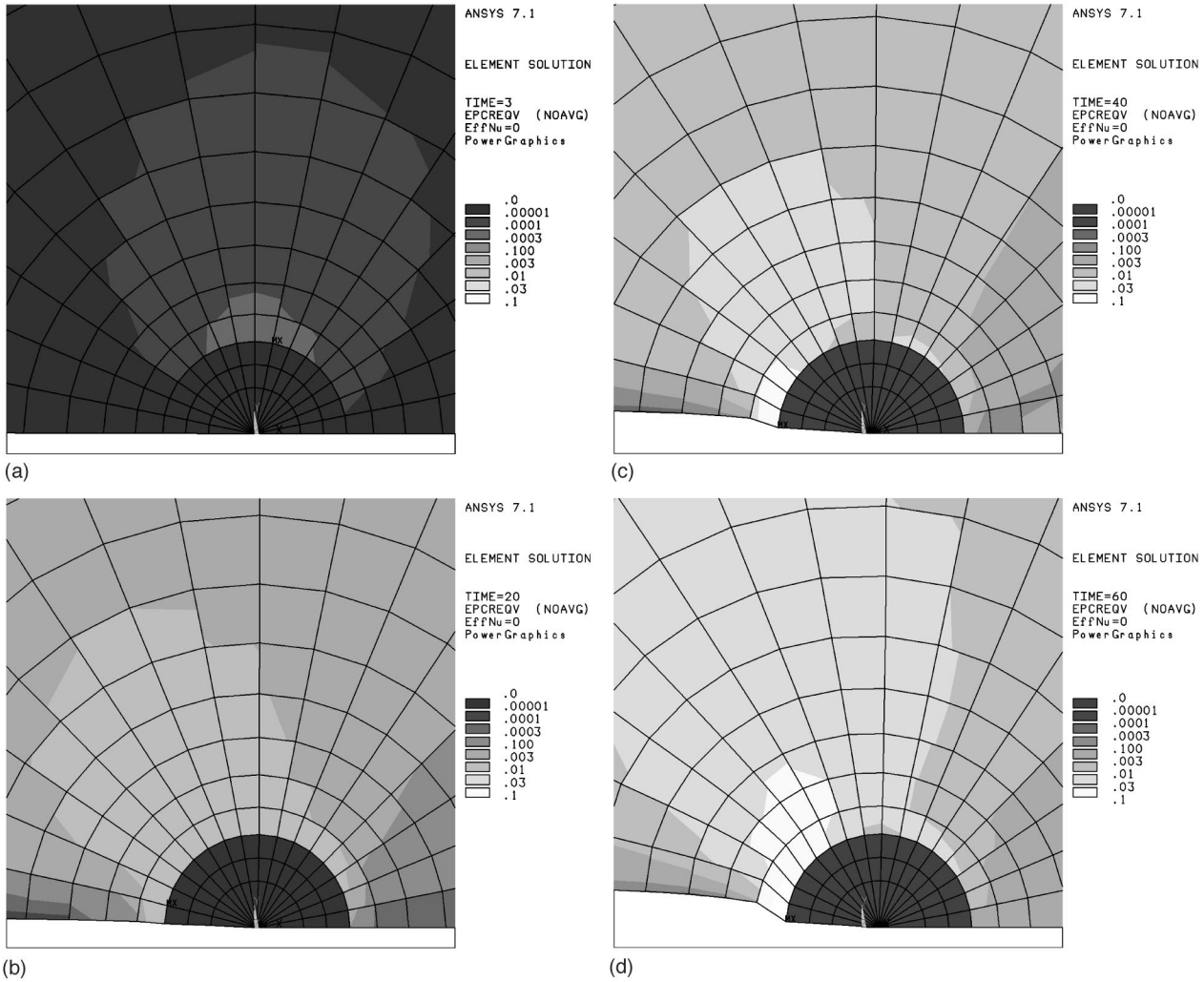

FIG. 9. The von Mises equivalent plastic strain at different applied loads (a) 0.3 MPa m$^{1/2}$, (b) 2 MPa m$^{1/2}$, (c) 4 MPa m$^{1/2}$, (d) 6 MPa m$^{1/2}$) of the simulation with $\dot{K} = 0.1$ MPa m$^{1/2}$/s and $T = 285$ K, i.e., immediately after the BDT. The color scales for the stress contours are identical in each plot. The plastic zone expands from the highly stressed regions toward the crack plane. Maxima (MX) of the plastic strain are indicated in each graph.

toward the crack plane is not complete. In these cases the load is transmitted to the elastic zone by the material in the vicinity of the crack plane, which behaves almost elastically. Only when this load transmission is delayed or even interrupted by viscoplastic relaxation the elastic zone, and thus the crack tip, is efficiently shielded from the applied load. Since the time needed for the viscoplastic zone to expand toward the crack plane depends on temperature, the whole process is thermally activated as described by Eq. (12).

The size of the elastic zone has a quite pronounced influence on the resulting fracture toughness and BDT temperature. A smaller elastic zone results in higher fracture toughnesses and lower BDT temperatures. In contrast, a larger elastic zone decreases the fracture toughness and increases the BDT temperature. This is expected because the stresses are higher closer to the crack tip, and therefore the plastic relaxation at the perimeter of a smaller elastic zone is faster.

V. DISCUSSION

We start the discussion with a critical assessment of the limitations and simplifications of both numerical models in the light of results published in the literature. The comparison between the complementary DDD and continuum models shows a consistent scaling behavior, which is interpreted in the following. We conclude with a model of the BDT in single crystals and by giving the prevailing rate-limiting processes in the different temperature regimes.

A. Limitations of the employed models

The observation that the total force on the dislocation population on a single slip plane can be expressed as a product of powers of the number of dislocations and of the local stress intensity factor has been motivated by a physical reasoning, but certainly this has to be subject to further investigations. A comparison with experimental data would be of special interest and is possible via Eq. (7) which states a relation between the fracture toughness and the total number of dislocations in form of a power law. The empirical constants of this power law are only functions of the elastic properties of a material and the Burgers vector, but not of external state variables or the dislocation velocity law.

The proportionality between the dislocation nucleation rate and dislocation velocity is nontrivial even under the prerequisite that dislocation nucleation occurs easily and homogeneously along the crack front. If dislocation nucleation itself is a thermally activated process, it is possible—depending on the activation energy—that dislocation nucleation is the rate limiting process. In this case, the apparent activation energy for crack-tip plasticity can be assumed to be related to the activation energy of dislocation *nucleation*, rather than to the activation energy for dislocation *motion*. There is, however, experimental evidence that in tungsten single crystals dislocation mobility is in fact the rate limiting process, at intermediate and at elevated temperatures.[23]

The number of dislocations below which the crack is still considered sharp has been chosen such that the BDT temperature at the given loading rate matches roughly that of experimental data. The resulting crack tip blunting of all $N_d^{\mathrm{crit}}=3900$ dislocations is $r_t=0.5\ \mu$m. Since the values of $k_{c,s}$ and $k_{c,b}$ must be equal at this blunting radius, the rupture strength of the material follows from Eq. (3) as $R_c=E/123=3.2$ GPa, which is an order of magnitude smaller compared with the usual estimate $R_c=E/10$. However, this value agrees reasonably well with fracture toughness measurements of tungsten specimens with a blunt notch at low temperatures, which yields $R_c=1.7$ GPa as rupture strength according to Eq. (3) (Ref. 29) and is also consistent with breaking stresses reported for low-temperature tensile tests on tungsten single crystals.[20] For dislocation-free silicon single crystals Gally and Argon[2] estimated the total number of nucleated dislocations at the BDT as $N_d=14\,500$ and estimated a critical blunting radius on the order of 1 to 5 μm, thus obtaining still higher figures than in this work. However, it is noted here that in the simple 2D model employed here all dislocations are perfectly shielding and blunting the crack tip, a situation that is unlikely to be reached under experimental conditions.

The simplicity of the model and especially that of the failure criterion applied here does not allow for the calculation of quantitative fracture toughness-temperature curves. Our treatment of crack-tip blunting merely shows that shielding of a crack tip in combination with blunting can cause a transition to ductile behavior, while crack-tip shielding alone always results in final fracture and thus in semibrittle behavior.

More sophisticated approaches by Deshpande *et al.*[18,30] describe crack-tip opening, crack-tip blunting, and crack advance with cohesive zone models. The combination of DDD with a finite element model allows these authors to describe the effect of crack-tip blunting quantitatively. With the help of this model the interaction of crack-tip blunting and elastic shielding with crack advance were studied under static and cyclic loading conditions. This work is focused on intrinsically ductile materials, where a large number of dislocation sources is homogeneously distributed within the material and dislocations glide easily. Therefore many slip planes become activated and a plastic zone develops that can be compared with the predictions of continuum crystal plasticity. This work thus contrasts work on the BDT, where intrinsically brittle materials with a lack of dislocation sources and low dislocation mobility are investigated. In fact, Kysar[11] showed by dimensional analysis, that dislocation nucleation in virtually defect-free materials should occur preferably at the crack tip.

The 2D elastic-viscoplastic model of crack-tip plasticity that has been adapted to tungsten showed basically the same features as the original work on silicon,[12] namely, a very sharp BDT with a well-defined activation energy. The main difference to this work lies in the applied constitutive relation for viscoplastic material behavior, where we employed a temperature dependent stress exponent to adapt the constitutive law to tungsten. This temperature dependent stress exponent effectively reduces the apparent activation energy of the BDT, as described in Sec. III.

A closer investigation of the loading of the elastic zone embedded in the viscoplastic material shows that the plastic

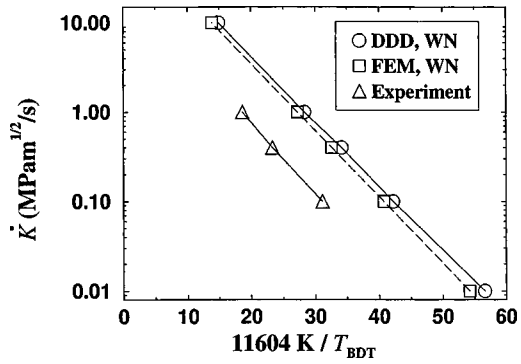

FIG. 10. Arrhenius plot of the loading rate versus the inverse BDT temperature for data obtained from DDD and FEM models as well as from experiment (Ref. 23).

zone expands around the elastic zone and the region of the highest plastic strains moves toward the crack surface. Simulations resulting in ductile behavior always show that the highest plastic strains occur close to the corner of the elastic zone on the crack plane. The evolution of the plastic zone from the region of highest shear stresses toward the crack plane yields an effective blunting of the crack tip and leads to the BDT. The absence of a semibrittle regime in this model is explained by the absence of plastic shielding at low and intermediate temperatures, due to the spatial separation of the plastic zone from the crack tip. This shielding, in contrast, is taken into account by the 2D-DDD model, which consequently shows a pronounced semibrittle regime.

B. Interpretation of the scaling behavior

For the simple dislocation model of crack-tip plasticity considered in this work the BDT occurs at a constant critical number of nucleated dislocations (yielding a critical blunting radius) and therefore at a constant fracture toughness [cf. Fig. 3 and Eq. (7)]. Consequently, the activation energy of the BDT derived by the scaling procedure is identical to the activation energy obtained by an Arrhenius analysis of the BDT temperatures at different loading rates (see Fig. 10). However, it seems interesting to note that both analyses applied to experimental data of tungsten[23] also yields identical activation energies for crack-tip plasticity and for the BDT. For this experimental data both activation energies amount to $Q_{\mathrm{scal}}=0.18$ eV.

The viscoplastic continuum model does not show a pronounced semibrittle regime, such that only an activation energy for the BDT can be determined by an Arrhenius plot, as shown in Fig. 10. It is seen that although the quantitative values for the BDT temperatures for given loading rates differ somewhat from model to model and also from model to experiment the slopes of the curves and thus the activation energies for the BDT are almost identical. Of course the value of this quantity is strongly influenced by several model parameters, however, the Arrhenius scaling of the inverse BDT temperature with loading rate is a non-trivial result of our models. Moreover, the good agreement of the activation energies of these complementary models shows, that the scaling behavior is a generic, model independent feature of the rate depend plastic deformation of the crack-tip region. It is noted here that these results on thermal activation of the BDT temperature are in excellent agreement with the results of an analytical viscoplasticity model by Argon *et al.*,[13] see also Fig. 7 in Ref. 14, which is based on different assumptions and approximations.

The activation energy for crack-tip plasticity and the BDT in tungsten—as derived from the scaling procedure—is one order of magnitude lower than the activation energy for screw dislocation motion, which is usually considered to be the rate determining process in bcc metals. However, the total plastic strain needed to achieve a BDT in the viscoplasticity model remains below 10%. This amount of plastic strain in bcc materials can be ascribed to microplasticity, i.e., plasticity that occurs without the large scale motion of screw dislocations. If the crack tip is a fertile source of dislocations, whose screw parts only move in the highly stressed crack-tip region, creating nonscrew dislocations on blunting slip planes, plastic strains of 5–10 % seem to be achievable without the motion of screw dislocations in the far field.

The stress dependence of the thermal activation term in the velocity law (2) requires an effective stress of $\tau \approx \tau_0/2$ to explain the experimentally observed apparent activation energy for crack-tip plasticity that is an order of magnitude smaller than the activation energy for screw dislocation motion. This defines a length scale around the crack tip on which screw dislocations can be considered mobile. With typical values for tungsten, this length scale is on the order of 30 μm at the BDT. The actual plastic zone size at the BDT is at least one order of magnitude larger, which shows that the motion of screw dislocations cannot be the limiting factor for crack-tip plasticity in tungsten. Consequently the DDD simulations based on the mobility of screw dislocations (WS) show much larger values for the BDT temperature and also for the activation energy of crack tip plasticity (see Sec. III). This reasoning also justifies the use of the dislocation velocity law for non-screw dislocations in our models.

A practical use of the derived scaling relation is that for a given material the fracture toughness in the semibrittle regime can be predicted for different temperatures and loading rates. This requires the knowledge of a fracture toughness-temperature curve for a single loading rate and the apparent activation energy for crack-tip plasticity, which can be derived from single experiments for at least two different loading rates. Such a model-based extrapolation of experimental data can save a large number of experiments and, moreover, the fracture toughness can be predicted for temperatures or loading rates that are not easily established in experiments.

C. Model for the BDT

The results presented in this work allow us to derive a rheological model of the BDT as shown in Fig. 11. The stiff breakable spring S_1 is loaded in series with the dashpot D. Spring S_2, which is unbreakable and less stiff than S_1, is loaded parallel to the system $D-S_1$. Spring S_1 can be rationalized as the elastic zone around the crack tip. The dashpot consequently relates to the viscoplastic zone. Spring S_2 cor-

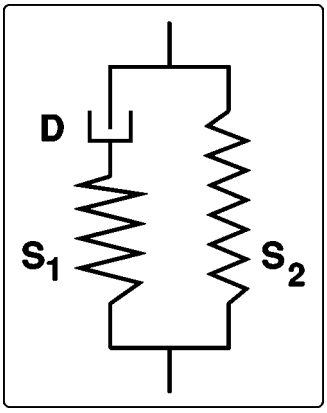

FIG. 11. Rheological model of crack-tip plasticity: S_1 represents a stiff, breakable spring, S_2 is a less stiff, unbreakable spring, and D is a dashpot.

responds to the elastic material around the viscoplastic zone for which the deformation rate is virtually zero. This spring is considered unbreakable and can transmit any given load. The stress that drives the viscoplastic relaxation is always equal to the stress transmitted by spring S_1. If the stress relaxation in the dashpot occurs slowly, almost all the load is transmitted to the crack tip (spring S_1) which fails at a given load. If, in contrast, the plastic strain of the dashpot increases with a sufficient rate, the surrounding elastic material (spring S_2) transmits the main part of the applied load and thus relieves the crack tip.

The loading of "spring" and "dashpot" of the real crack problem occurs in a geometrically complex manner. However, the key of this rheological model is that the BDT occurs when the stress relaxation in the plastic zone takes place with the same rate at which the applied load is increased, which should also hold for the real case. The rate of the relaxation depends on temperature and stress, as described by Eq. (12). The maximum stress that can occur is given by the failure criterion. Thus, the BDT takes place if the temperature is high enough such that the rate of plastic relaxation at or below the failure stress (or the critical local stress intensity factor for crack advance) keeps pace with the applied loading rate. As motivated by the DDD results discussed above crack-tip blunting is a dominant factor for the transition to ductile behavior, because it increases the effective fracture toughness and thus allows the surrounding material to deform at a higher rate.

In previously published work[16] we have shown that the dislocation nucleation rate limits plastic relaxation of the crack tip at low temperatures. Together with the present work it is now possible to name the rate limiting factors of the BDT in three stages referring to three different temperature regimes: (i) nucleation controlled regime at low temperatures; (ii) mobility controlled regime at intermediate and high temperatures; and (iii) transition to ductility by crack-tip blunting at the BDT temperature. Crack-tip plasticity and the BDT itself can be described as thermally activated processes with identical activation energies. The formulation of the force balance at the crack tip shows how this activation energy is related to the activation energy of dislocation motion.

The models presented in this work describe the plastic zone in a single crystal. The reasoning derived from the findings is consequently also valid only for the case of single crystals. When the grain size of a polycrystal becomes smaller than the plastic zone, i.e., smaller than 1 mm, the interaction of dislocations with the grain boundaries will effectively block the dislocation and thus disturb the buildup of an inverse pileup. For such fine grained material the scaling relations derived in the present work will not be valid. Even more so, because grain boundaries may also change the brittle fracture path and dislocation-grain boundary interactions leads to microcrack nucleation and may thereby yield a completely different failure mode.

VI. CONCLUSIONS

The modeling of crack-tip plasticity by discrete dislocation dynamics models on one hand and by elastic-viscoplastic continuum models on the other hand, reveal the importance of crack-tip blunting for the brittle-to-ductile transition (BDT). The discrete dislocation model yields a good description of the early phases of crack-tip plasticity and the semibrittle regime, whereas crack-tip blunting and the resulting BDT are modeled in a simplistic manner. The continuum plasticity model, in contrast, exhibits quite naturally a transition from brittle to ductile behavior, but the semibrittle regime is not well captured in this model. However, the results of both complementary models show a consistent scaling behavior of crack-tip plasticity and the BDT temperature that is also in good agreement with experimental data.

The theoretical analysis of this scaling behavior reveals that crack-tip plasticity and fracture toughness in the semibrittle regime as well as the BDT temperature are thermally activated with a constant activation energy. This activation energy for crack-tip plasticity and the BDT is identical with or—depending on the stress dependence of the dislocation velocity—at least closely related to the activation energy for dislocation motion. An analytical scaling relation for loading rate and temperature at points of constant fracture toughness is derived based on the treatment of crack-tip plasticity as a thermally activated process. This scaling relation also describes experimental results very well, and thus can be employed for a model-based extrapolation of fracture toughnesses of engineering materials.

*Email address: hartmaier@mf.mpg.de

[1] S. G. Roberts, A. S. Booth, and P. B. Hirsch, Mater. Sci. Eng., A **176**, 91 (1994).
[2] B. Gally and A. Argon, Philos. Mag. A **81**, 699 (2001).
[3] J. R. Rice and R. Thomson, Philos. Mag. **29**, 73 (1974).
[4] R. Thomson, in *Solid State Physics*, edited by H. Ehrenreich and D. Turnbull (Academic Press, New York, 1986), Vol. 39, pp. 1–129.
[5] M. Brede and P. Haasen, Acta Metall. **36**, 2003 (1988).
[6] J. Weertman, I.-H. Lin, and R. Thomson, Acta Metall. **31**, 473 (1983).
[7] P. B. Hirsch, S. G. Roberts, and J. Samuels, Proc. R. Soc. London, Ser. A **421**, 25 (1989).
[8] J. W. Hutchinson, J. Mech. Phys. Solids **16**, 13 (1968).
[9] J. R. Rice and G. F. Rosengren, J. Mech. Phys. Solids **16**, 1 (1968).
[10] S. Flouriot, S. Forest, G. Cailletaud, A. Koster, L. Remy, B. Burghardt, V. Gros, S. Mosset, and J. Delautre, Int. J. Fract. **124**, 43 (2003).
[11] J. Kysar, J. Mech. Phys. Solids **51**, 795 (2003).
[12] V. R. Nitzsche and K. J. Hsia, Mater. Sci. Eng., A **176**, 155 (1994).
[13] A. Argon, G. Xu, and M. Ortiz, in *George R. Irwin Symposium on Cleavage Fracture*, edited by K. Chan (Minerals, Metals and Materials Society, Warrendale, PA, 1997), pp. 125–135.
[14] A. Argon, J. Eng. Mater. Technol. **123**, 1 (2001).
[15] I.-H. Lin and R. Thomson, Acta Metall. **34**, 187 (1986).
[16] A. Hartmaier and P. Gumbsch, J. Comput.-Aided Mater. Des. **6**, 145 (1999).
[17] A. Hartmaier and P. Gumbsch, Philos. Mag. A **82**, 3187 (2002).
[18] V. Deshpande, A. Needleman, and E. V. der Giessen, Acta Mater. **51**, 1 (2003).
[19] A. Seeger and B. Šesták, Z. Metallkd. **69**, 195 (1978); **69**, 355 (1978); **69**, 425 (1978).
[20] D. Brunner, Mater. Trans., JIM **41**, 152 (2000).
[21] H. Schadler, Acta Metall. **12**, 861 (1964).
[22] U. F. Kocks, A. S. Argon, and M. F. Ashby, in *Progress in Materials Science*, edited by B. Chalmers, J. W. Christian, and T. B. Massalski (Pergamon Press Ltd., Oxford, UK, 1975), Vol. 19.
[23] P. Gumbsch, J. Riedle, A. Hartmaier, and H. F. Fischmeister, Science **282**, 1293 (1998).
[24] A. Hartmaier and P. Gumbsch, in *Continuum Scale Simulation of Engineering Materials: Fundamentals-Microstructures-Process Applications*, edited by D. Raabe, F. Roters, F. Barlat and L.-Q. Chen (Wiley-VCH, Weinheim, 2004), pp. 413–428.
[25] J. Riedle, P. Gumbsch, and H. F. Fischmeister, Phys. Rev. Lett. **76**, 3594 (1996).
[26] P. Gumbsch, J. Mater. Res. **10**, 2897 (1995).
[27] V. G. Glebovsky, B. M. Shipilevsky, I. V. Kapchenko, and V. V. Kirzyko, J. Alloys Compd. **184**, 297 (1992).
[28] V. G. Glebovsky, I. V. Kapchenko, and B. M. Shipilevsky, J. Alloys Compd. **184**, 205 (1992).
[29] J. Riedle, Ph.D. thesis, Universität Stuttgart, 1995.
[30] V. Deshpande, A. Needleman, and E. V. der Giessen, Acta Mater. **49**, 3189 (2001).